Thermochimica Acta 496 (2009) 129–135

Contents lists available at ScienceDirect

Thermochimica Acta

journal homepage: www.elsevier.com/locate/tca

Thermodynamics of the complexation of Hg(II) by cysteinyl peptide ligands using isothermal titration calorimetry

Maria Ngu-Schwemlein*, John K. Merle, Patrick Healy, Stefanie Schwemlein, Sade Rhodes

Department of Chemistry, Winston-Salem State University, Winston-Salem, NC 27110, USA

ARTICLE INFO

Article history:
Received 13 May 2009
Received in revised form 14 July 2009
Accepted 20 July 2009
Available online 28 July 2009

Keywords:
Cysteine S-donor peptide ligands
Mercury (II) binding
Isothermal titration calorimetry
Stern–Volmer plots

ABSTRACT

The present study was undertaken to better understand the complexation of mercury (II) by cysteine, histidine, tryptophan, and their di- and tri-peptides. Their mercury (II) binding affinities and associated thermodynamic parameters are evaluated by isothermal titration calorimetry. Cysteine S-donor atoms form the strongest complexes, which can be attributed to a more exothermic Hg–S soft acid and soft base interaction. These thiol S-donor peptide ligands show two sequential binding for mercury (II). Their stability constants for the first binding (10^8 M^{-1} to $>10^{10}$ M^{-1}) are largely due to favorable contribution of the enthalpy term to the free energy of complexation. As more mercury (II) ions are added, this enthalpy contribution decreases and the free energy of the second binding (10^5 M^{-1} to 10^6 M^{-1}) is partially compensated by the entropy term. The dependency of the fluorescence intensity for these peptides on mercury (II) concentration shows two different Stern–Volmer plots, which corroborates the calorimetric data and supports the formation of two types of stable complexes.

1. Introduction

Clinical chelation therapy of mercury poisoning [1] generally uses thiol compounds such as dimercaptosuccinic acid (DMSA), dimercaptopropane-sulfonic acid (DMPS), and when necessary, cysteine (Cys) and *N*-acetylcysteine (NAC) for hemodialysis [2,3]. However, it has been shown that these are not well-optimized molecules for mercury chelation therapy [4]. For example, the catabolism of Cys in the gastrointestinal tract and the blood plasma limits its use in chelation therapy. Furthermore, there is evidence of an increased level of mercury in the brain associated with post-exposure treatment with NAC. The entry of Cys S-conjugates of mercury (II) into cells, such as brain cells, has been ascribed to the molecular mimicry of these complexes, which serve as substrates for amino acid transporters into cells. Bridges and Zalups showed that Cys S-conjugates of inorganic mercury and the amino acid cystine are both transported by the same amino acid transport system via a mechanism whereby the complex acts as a structural and/or functional homologue of cystine [5,6]. Molecular mimicry was first implicated by Clarkson and Aschner in the cellular uptake of Cys S-conjugate of methylmercury, which mimics the amino acid, methionine, at the site of a membrane amino acid transporter to gain access to the intracellular compartment of cells [7,8]. Although the mechanism for the transport of Cys S-conjugates of mercuric ions via the lipophilic blood–brain barrier has not been substantiated by the isolation of such carrier proteins and their binding sites for these complexes as well as their respective amino acid substrates, molecular mimicry remains a logical explanation for the intrusive entry of Cys S-conjugates of mercury (II) into cells. As such, it is worthwhile to investigate the complexation of mercury (II) by di- or tri-peptides containing Cys residue(s). These mercury (II) and Cys-peptide complexes should evade transportation across the blood–brain barrier via an amino acid carrier by virtue of their size, structural differences, and their lower values of similarity indexes compared to the mercury (II) and Cys or amino acid complexes.

We evaluated the binding affinities and associated thermodynamic parameters of the interactions of mercury (II) with the di- and tri-peptides of Cys containing histidine (His), for its imidazole-*N*-donor atom, and tryptophan (Trp), for its potential electrostatic cation–pi interactions and concurrent intrinsic fluorogenic properties. We anticipate improved chemical stability towards peptidases by using alternating D- and L-stereochemistry. Additionally, we postulate that these structurally larger di- and tri-peptides of Cys S-conjugates of mercury (II) will not readily gain access to the intracellular compartments of cells via amino acid transporter systems by molecular mimicry. These Cys S-donor peptide ligands could be promising alternatives for Cys and NAC as mercury (II) chelation agents if they exhibit tight binding affinity for mercury (II). The objectives of this study are (i) to compare the formation constants and their associated thermodynamic parameters of mercury (II) complexes of Cys, His, Trp, and their heterochiral di- and tri-

* Corresponding author at: Department of Chemistry, W.B. Atkinson Science Bldg., Rm. 309, Winston-Salem State University, Winston-Salem, NC 27110, USA. Tel.: +1 336 750 2919; fax: +1 336 750 2549.
E-mail address: Schwemleinmn@wssu.edu (M. Ngu-Schwemlein).

0040-6031/$ – see front matter © 2009 Elsevier B.V. All rights reserved.
doi:10.1016/j.tca.2009.07.010

peptides, (ii) to assess the relative effectiveness of these peptide ligands in mercury (II) complexation, and (iii) to provide a rationale in using these peptide ligands in mercury (II) chelation therapy.

The present study was undertaken to better understand the complexation of mercury (II) by Cys and their di- and tri-peptides with Trp and His. We report here the thermodynamic parameters, enthalpy (ΔH), entropy (ΔS), and free energy (ΔG), including the binding constant (K_a), for the interactions between these Cys ligands and mercury (II) by isothermal titration microcalorimetry (ITC) so as to obtain more insight into the origin of binding affinity and specificity in these systems. Specific mercury (II) interactions by the fluorogenic peptide ligands are also assessed by steady state fluorescence spectroscopy [9a]. Standard Stern–Volmer formalism and the dependence of fluorescence intensity on mercury (II) concentrations are evaluated and compared with complex formations as measured by calorimetry. The results of these calorimetric and spectroscopic studies of Cys S-conjugates of mercury (II) show that Cys S-donor peptide ligands are viable alternatives of Cys and *N*-acetylcysteine (NAC) as mercury (II) chelation agents.

2. Experimental

2.1. Materials and methods

All chemicals were obtained from commercial suppliers and used without further purification. Di- and tri-peptides of cysteine, histidine, and tryptophan (>95% purity) were purchased from AnaSpec Incorporated, California, USA. All other chemicals, including dimercaptosuccinic acid (98%), dimercaptopropane-sulfonic acid (95%), cysteine (99.5%), histidine (99.5%), tryptophan (99.5%), mercury (II) perchlorate (>98% purity), were purchased from Sigma–Aldrich Chemical Company.

2.2. Isothermal titration calorimetry

Microcalorimetric titrations of peptides with metal ions were conducted by isothermal titration microcalorimetry (ITC) using a Microcal VP-ITC Instrument (Northampton, MA, USA). Experiments were carried out at 30 °C in 10 mM MOPS at pH 7.4. DMSA, DMPA, amino acids, and peptide concentrations ranged from 0.1 mM to 0.15 mM (1.34 mL sample cell), while the metal ion concentrations varied from 1.0 mM to 3.0 mM in the syringe. These solutions were degassed for 5 min by using the Microcal Thermo Vac degassing unit, and then stored under nitrogen to minimize sample oxidation. Automated titrations were conducted until saturation, up to a mercury (II)/peptide mole ratio of about 3–7. Each mercury (II)/ligand type experiment was repeated at least three times. Heats of dilution and mixing for each experiment were measured by titrating the mercury (II) solution into 10 mM MOPS at pH 7.4. The effective heat of each peptide metal ion interaction was corrected for dilution and mixing effects. These heats of bimolecular interactions were obtained by integrating the peak following each injection of metal ion. The data were analyzed using the Microcal Origin 7.0 software (Microcal Software, Inc.) to determine the molar enthalpy change for binding, ΔH^o, and the corresponding binding constant, K_a. The molar free energy of binding, ΔG^o, and the molar entropy change, ΔS^o, were derived from the fundamental equations of thermodynamics, $\Delta G^o = -RT \ln K_a = \Delta H^o - T(\Delta S^o)$.

2.3. Steady state fluorescence spectroscopy

Fluorescence spectroscopy measurements were carried out on a Varian CARY Eclipse Spectrofluorometer (California, USA), equipped with a thermostated cell holder. The fluorescence spectra were recorded at 25 °C using 1×10^{-5} M peptide solutions in a 3 mL quartz cell that has a path length of 1 cm. The excitation

Table 1
Thermodynamic parameters of mercury (II) binding to DMSA, DMPS, Cys, His, Trp and the di- and tri-peptides of Cys with Trp and/or His[a,b,c].

	Compounds	K_a (M^{-1})	ΔH (kJ mol^{-1})	ΔG (kJ mol^{-1})	ΔS (J K^{-1} mol^{-1})
1	DMSA	$(2.7 \pm 0.1) \times 10^9$	−29.4 ± 0.6	−13.1 ± 0.1	−54 ± 2
		$(1.0 \pm 0.3) \times 10^6$	−13.3 ± 1.0	−8.3 ± 0.2	−17 ± 4
2	DMPS	$(2.0 \pm 0.4) \times 10^9$	−31.8 ± 0.7	−12.6 ± 0.03	−63 ± 2
		$(1.1 \pm 0.1) \times 10^7$	−22.7 ± 0.7	−9.6 ± 0.03	−43 ± 2
3	Cys	$(5.7 \pm 2.6) \times 10^{11}$	−30.3 ± 0.3	−16.0 ± 0.5	−48 ± 2
		$(8.4 \pm 1.7) \times 10^6$	−14.2 ± 0.1	−9.6 ± 0.1	−15 ± 1
4	His	$(7.1 \pm 1.5) \times 10^7$	−6.8 ± 0.1	−10.9 ± 0.1	13.3 ± 0.8
		$(1.9 \pm 0.1) \times 10^5$	−8.2 ± 0.2	−7.3 ± 0.1	2.8 ± 0.6
5	Trp	$(9.9 \pm 0.5) \times 10^4$	−4.6 ± 0.1	−6.9 ± 0.03	7.7 ± 0.3
6	D-Trp-His	$(7.4 \pm 0.9) \times 10^5$	−10.1 ± 0.2	−8.1 ± 0.01	−6.3 ± 0.6
7	D-Trp-Cys	$(7.6 \pm 0.6) \times 10^{10}$	−26.4 ± 0.4	−14.5 ± 0.6	−39 ± 2
		$(1.2 \pm 0.1) \times 10^6$	−8.3 ± 0.3	−8.5 ± 0.1	−0.7 ± 0.07
8	Trp-D-Cys	$(3.0 \pm 0.3) \times 10^{10}$	−31.3 ± 0.3	−14.5 ± 0.05	−55.4 ± 0.6
		$(1.4 \pm 0.2) \times 10^6$	−10.2 ± 0.2	−8.5 ± 0.1	−5.4 ± 0.9
9	Trp-Cys	$(2.1 \pm 0.9) \times 10^{10}$	−31.5 ± 0.7	−14.1 ± 0.4	−57.2 ± 3.0
		$(5.9 \pm 0.4) \times 10^5$	−9.9 ± 0.05	−8.0 ± 0.04	−6.4 ± 0.05
10	His-D-Trp-Cys	$(3.5 \pm 0.1) \times 10^8$	−8.1 ± 0.1	−11.9 ± 0.03	12.3 ± 0.3
		$(5.6 \pm 0.4) \times 10^5$	−15.0 ± 0.1	−8.0 ± 0.06	−23.2 ± 0.2
11	Cys-D-Trp-His	$(2.5 \pm 0.9) \times 10^8$	−7.7 ± 0.4	−11.5 ± 0.3	12.5 ± 0.6
		$(1.3 \pm 0.04) \times 10^6$	−13.7 ± 0.04	−8.4 ± 0.02	−17.4 ± 0.2
12	His-Trp-Cys	$(5.3 \pm 1) \times 10^8$	−9.3 ± 0.1	−11.9 ± 0.03	9.1 ± 0.09
		$(6.2 \pm 0.2) \times 10^5$	−14.6 ± 0.2	−8.0 ± 0.06	−21.8 ± 0.5
13	Cys-D-Trp-Cys	$(2.5 \pm 0.8) \times 10^{10}$	−27.1 ± 0.2	−14.1 ± 0.4	−42.0 ± 1.5
		$(2.4 \pm 0.2) \times 10^6$	−21.2 ± 0.2	−8.0 ± 0.04	−40.7 ± 0.6

[a] Values correspond to the mean of three experiments and the standard error.
[b] Mercury (II) perchlorates.
[c] Some of these values exceed the detection limits of ITC ($10^2 < K_a < 10^{10}$ M^{-1}).

wavelength was 280 nm and fluorescence emission at 355 nm was used in quenching studies. The excitation and emission slit widths were fixed at 5 nm or 10 nm. The dependency of the fluorescence intensity on quencher concentration was analyzed by the Stern–Volmer equation: $F_0/F = 1 + K_{SV}[Q]$, where F_0 and F are the fluorescence intensities in the absence and presence of the quencher, respectively, K_{SV} is the Stern–Volmer constant, and [Q] is the concentration of the quencher [9b]. When the dependence of F_0/F on [Q] is linear, K_{SV} can be associated with either dynamic (K_D) or static processes (K_S). Combined dynamic and static quenching is characterized by un upward curvature, concave towards the *y*-axis, and can be described by the following modified form of the Stern–Volmer equation, which is second order in [Q]: $F_0/F = (1 + K_D[Q])(1 + K_S[Q])$. Static and dynamic quenching can be distinguished by their different dependencies on temperature [9b]. Higher temperature will enhance diffusion rates, which will increase the gradient of the Stern–Volmer plots and result in larger K_D values. Conversely, higher temperature will result in the dissociation of weakly bound complexes, and hence result in smaller K_S values. Variable temperature Stern–Volmer plots were conducted at 25 °C, 35 °C and 40 °C to distinguish between static and dynamic quenching. Additionally, the degree of static quenching was assessed by these variable temperature Stern–Volmer plots. Tightly bound complexes are not readily dissociated at higher temperature and hence will not show appreciable changes in Stern–Volmer plots with increasing temperature.

3. Results and discussion

3.1. Isothermal calorimetric studies

The binding affinity values of DMSA, DMPA, Cys, His, Trp and the di- and tri-peptides of Cys with Trp and/or His (compounds

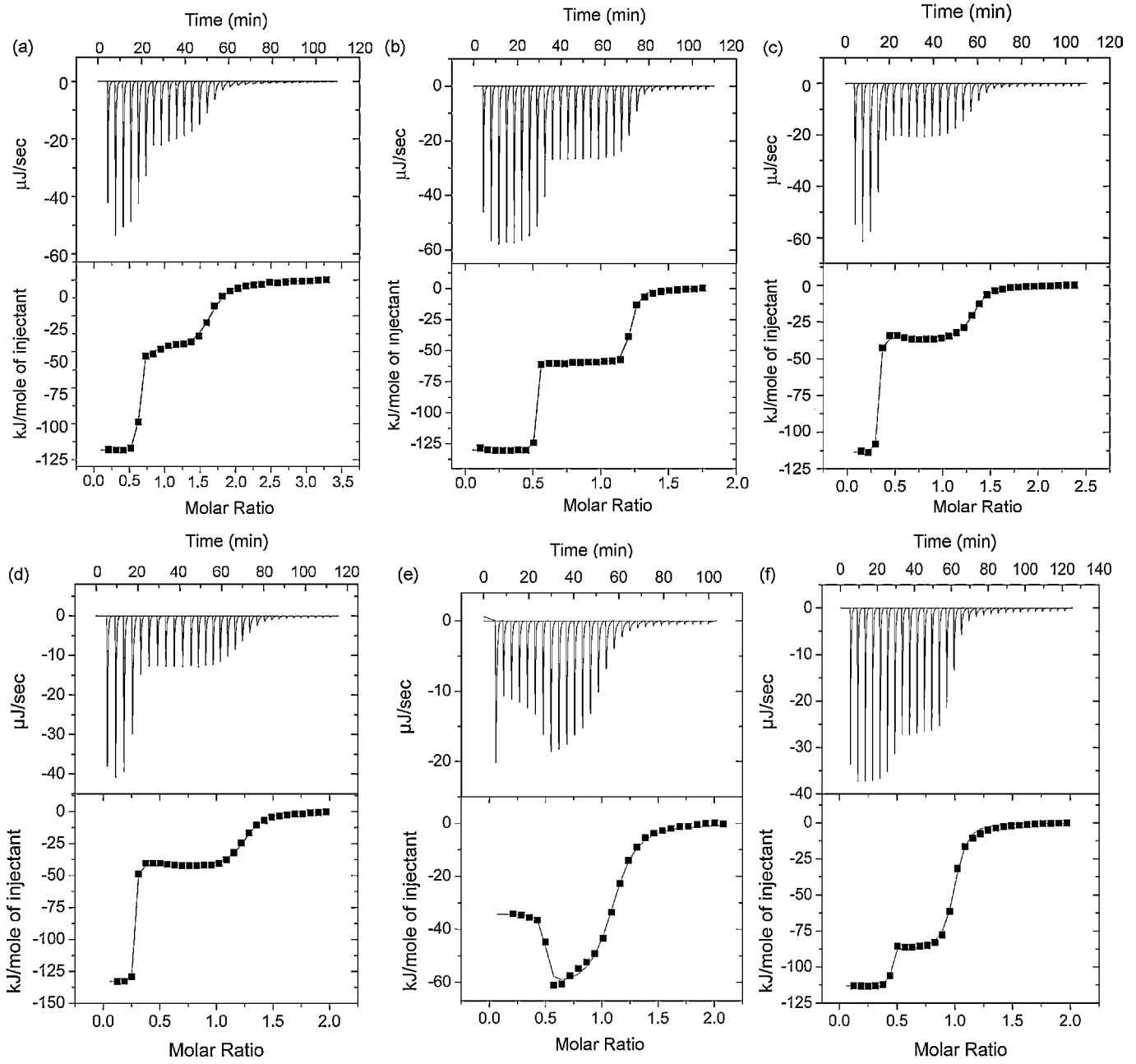

Fig. 1. ITC data curve of (a) DMSA, (b) Cys, (c) D-Trp-Cys, (d) Trp-D-Cys, (e) His-D-Trp-Cys, and (f) Cys-D-Trp-Cys, following titration with mercury (II). Raw ITC titration data (top panels). Binding isotherms (bottom panels) are derived from the data in the corresponding top panels following correction for dilution and mixing effects.

1–**13**) for mercury (II), and their associated thermodynamic parameters are summarized in Table 1. Fig. 1 shows the total measured heat associated with each titration of mercury (II), and the binding isotherms derived from the heat change following each titration for DMSA (**1**), Cys (**3**), D-Trp-Cys (**6**), Trp-D-Cys (**7**), His-D-Trp-Cys (**10**), and Cys-D-Trp-Cys (**13**). As previously reported for some cyclopeptides [10,11], these thiol S-donor ligands also exhibit two sequential bindings for mercury (II).

A strong exothermic association takes place at the beginning of each titration of mercury (II) into the thiol S-donor compounds (Fig. 1a–f). This clearly indicates the formation of Hg–S coordinate bond(s), as soft donor and soft acceptor interactions are typically strongly exothermic. Consequently, the thiol S-donor group acts as the primary ligating group or "anchor" for stable complex formation. At the beginning of the titration, the concentrations of the thiol ligands are relatively higher than that of mercury (II). Accordingly, the formation of the first complex would resemble an ML_2 complex, where M is the mercury (II) ion and L, the thiol S-donor ligand. An ML_2 complex would correspond to a mercury (II)/peptide molar ratio of 0.5. We postulate that the mercury (II) ion could be forming a linear, two coordinate complex, which would be consistent with the coordination chemistry of Hg^{2+} (d^{10}), a soft acid that has a tendency to form linear thiolate complexes with a coordination number of 2 [12,13]. Titration of additional mercury (II) to the ML_2 complex, where the mercury (II)/peptide molar ratio is greater than 0.5, is characterized by smaller $-\Delta H^o$ and $-\Delta S^o$ values. The second complex formation constants for these compounds (**1**, **3**, **6**, **7**, **8**, **10**, and **13**) ($K_{a''}$ values range from $5 \times 10^5\ M^{-1}$ to $8 \times 10^7\ M^{-1}$) (Table 1) are much weaker than their corresponding first formation constants ($K_{a'}$ values range from $2 \times 10^8\ M^{-1}$ to $>10^{10}\ M^{-1}$). It resembles complex formation with amine and/or carboxylate groups. However, since the exact complex type composition present in a given titrated solution is not known at this time, the involvement of mixed binding modes cannot be readily distinguished. We are in the progress of using density functional theory calculations to help identify the probable modes of complexation between mercury (II) and cysteine terminated peptides at mercury (II)/peptide molar ratios less than and greater than 0.5.

In contrast, the formation of mercury (II) complexes with His (**4**), Trp (**5**) and D-Trp-His (**6**) is characterized by a much smaller $-\Delta H^o$ value (Table 1). This can be rationalized by charge neutralization between a hard base donor and a soft acid acceptor and is consistent with N–Hg and/or O–Hg coordinate bond formation. The stability of these His–Hg^{2+} and Trp–Hg^{2+} complexes is supported by favorable entropy changes. The binding constants of these mercury (II) complexes ($K_{a'}$ values range from $7 \times 10^5\ M^{-1}$ to $7 \times 10^7\ M^{-1}$) are significantly lower than those involving the thiol S-donor ligands (Table 1).

Fig. 2 shows the binding constants of the peptide ligands for mercury (II) compared to that of their constituent amino acids, as well as the clinical chelators (DMSA and DMPA). Both DMSA and DMPA exhibit moderately high binding affinities for mercury (II), where their first binding constant values ($K_{a'}$) are $2.7 \times 10^9\ M^{-1}$ and $2.0 \times 10^9\ M^{-1}$, respectively. On the contrary, they exhibit a significantly weaker formation constant for the second complex formation, where $K_{a''}$ values are $1.0 \times 10^6\ M^{-1}$ and $1.1 \times 10^7\ M^{-1}$, respectively (Table 1 and Fig. 2). In comparison, the di-peptide, D-Trp-His, exhibits a moderate binding affinity ($K_{a'} = 7.4 \times 10^5\ M^{-1}$) for mercury (II). Its binding constant value is in between those of His ($K_{a'} = 7.1 \times 10^7\ M^{-1}$ and $K_{a''} = 1.9 \times 10^5\ M^{-1}$) and Trp ($9.9 \times 10^4\ M^{-1}$). In contrast, the corresponding Cys S-donor di-peptide, D-Trp-Cys, showed greater than a 10,000-fold increase in binding affinity for mercury (II) (Fig. 2). Remarkably, this very strong binding constant for mercury (II) is independent of the stereochemistry of the two component amino acid residues, Trp and Cys. All three di-peptides, D-Trp-Cys, Trp-D-Cys, and Trp-Cys exhibited very similar ITC binding isotherms for mercury (II) and consequently their derived formation constants. Similarly the set of tri-peptides His-D-Trp-Cys, Cys-D-Trp-His, and His-Trp-Cys, are alike in their formation constants with mercury (II) despite their structural differences in amino acid sequence and stereochemistry. However, these tri-peptides show a 100-fold decrease in their first binding affinity for mercury (II) ($K_{a'}$ values range from $2.5 \times 10^8\ M^{-1}$ to $5.3 \times 10^8\ M^{-1}$) compared to the di-peptides. Although each of these di- and tri-peptides consists of one Cys S-donor group, their initial interactions with mercury (II) are significantly different. This could be rationalized by the smaller Cys S-donor di-peptides, which can readily form a linear, two S-coordination complex with mercury (II) (ML_2). On the other hand, the larger tri-peptides consisting of double "anchors", a thiol S-donor atom of cysteinyl residue, and an imidazole-*N*-donor atom of histidyl residue, could form tetrahedral 2 N- and 2 S-coordinated ML_2 complexes, which are relatively less stable due to steric hindrance attributed by the imidazole-*N*-donor group(s). The binding constants for these tetrahedral coordinated complexes are significantly lower than the linear coordinated ones. In replacing the imidazole-*N*-donor with a second thiol S-donor, the tri-peptide Cys-D-Trp-Cys exhibited a 100-fold increase in binding affinity for

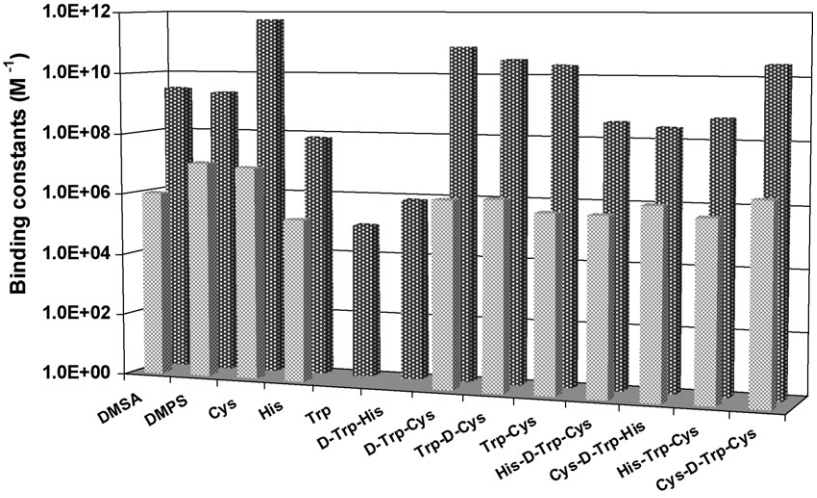

Fig. 2. Comparison of binding constants for mercury (II) complexation to DMSA, DMPS, Cys, His, Trp and the di- and tri-peptides of Cys with Trp and/or His (compounds **1**–**13**)(second binding constant, $K_{a''}$ — front row gray bars and first binding constant, $K_{a'}$ — second row bars).

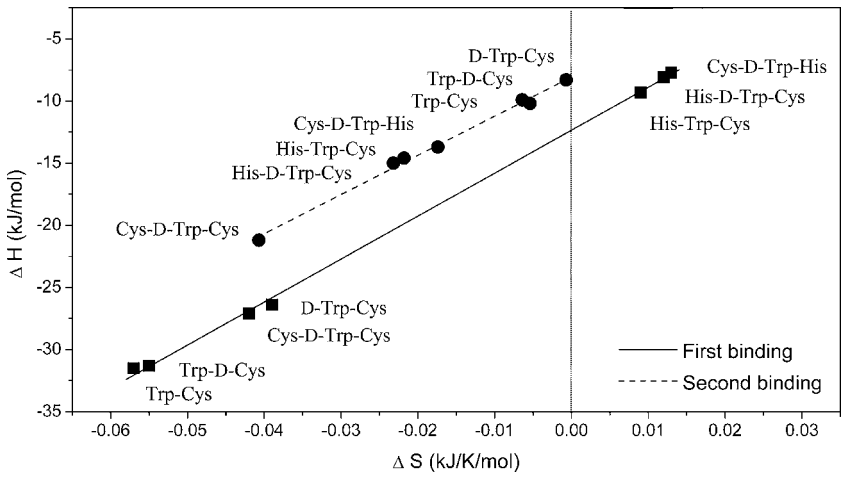

Fig. 3. Relationship between ΔH and ΔS for binding of mercury (II) to the thiol S-donor peptide ligands (compounds **7**–**13**).

mercury (II). This could be attributed to the smaller thiol S-donor group compared to the imidazole-*N*-donor group as well as the fact that Hg–S interactions are stronger than Hg–N interactions.

Although the free energies of binding vary only slightly within the individual sets of di- and tri-peptides for mercury (II), the corresponding enthalpies and entropies vary over a relatively larger range (Table 1). This trend is generally observed in complexation processes in which a decrease in enthalpy is associated with a decrease in complexation entropy [14]. The basis for this tendency is that a decrease in ΔH value arises from a stronger binding affinity between the complexing species, which in turn leads to the formation of a more rigid complex structure. As a result, a decrease in ΔH is compensated by a decrease in ΔS, a thermodynamic phenomenon which is referred to as an entropy–enthalpy compensation accompanying complex formations [15–17]. In an attempt to investigate this compensation during the Cys S-donor peptide ligands and mercury (II) complexation, ΔH was plotted against ΔS (Fig. 3). It appeared that ΔH is a linearly increasing function of ΔS for both the first and second binding associations between mercury (II) and the di- and tri-peptides; that is, $\Delta H^o = \alpha + T_c \Delta S^o$, where α is a constant for a given set of solvent conditions, and the slope T_c is called the compensation temperature. Lines of best fit for the correlations between ΔH_1 and ΔS_1 (first binding) yielded the linear regression line, $y = 344.8x - 12.33$ with coefficients of determination $r^2 > 0.99$, and ΔH_2 and ΔS_2 (second binding) yielded the linear regression line, $y = 315.2x - 8.07$, where $r^2 > 0.99$. However, it had been reported that an observed $\Delta H/\Delta S$ linear correlation does not suffice of itself to constitute a true or complete compensation effect [17]. Krug et al. suggested two conditions that are necessary, to support a chemical cause for entropy–enthalpy compensation: first, T_c, the compensation temperature must be significantly different from the experimental temperature; and second, the ΔH values should be linearly correlated with the ΔG values [18]. With a view to investigate the significance and validity of a compensation effect in the above system, we compared the slope T_c with our experimental temperature. The compensation temperature, slope T_c, for the first binding (344.8 K) and for the second binding (315.2 K), are significantly different from the experimental temperature, which is 303 ± 0.1 K. However, ΔH values did not show linear correlations with ΔG values. Although complete compensation cannot be established for the above system, it is likely that the compensation is partial.

Fig. 3 shows the correlation of ΔH with ΔS for these mercury (II) and peptide associations. The thiol S-donor di-peptide ligands (D-Trp-Cys, Trp-D-Cys, and Trp-Cys) and the tri-peptide containing two thiol S-donor groups, Cys-D-Trp-Cys, exhibit free energies of complexation that are largely driven by a favorable enthalpy term wherein their $\Delta H/\Delta S$ data pairs fall in the negative ΔH and negative ΔS quadrant of the plot. Likewise, the free energies of complexation for the weaker second binding associations of these peptides with mercury (II) are enthalpically driven. However, the tri-peptides containing only one thiol S-donor group (His-D-Trp-

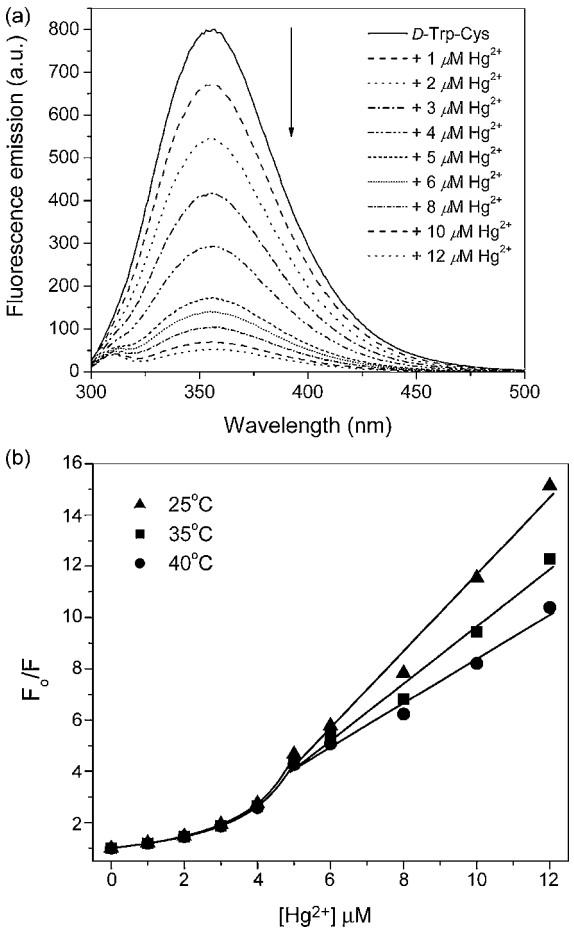

Fig. 4. (a) Fluorescence emission spectrum of 10 μM D-Trp-Cys in the absence and presence of increasing concentrations of mercury (II). (b) Stern–Volmer plots for mercury (II) quenching of D-Trp-Cys at 25 °C, 35 °C, and 40 °C.

Cys, Cys-D-Trp-His, and His-Trp-Cys) demonstrate free energies of complexation that are partially compensated by the favorably entropy term. Their $\Delta H/\Delta S$ data pairs for the first binding fall in the negative ΔH and positive ΔS quadrant of the plot (Fig. 3). This associated entropy increase could arise from the larger role of solvent reorganization and possibly larger conformational changes of the tri-peptides coupled with a more compact complex formation with internal rigidification [19] than the corresponding di-peptides. In general, as more mercury (II) ions are added, the enthalpy contribution decreases and the free energies of binding are compensated by the entropy term (Fig. 3).

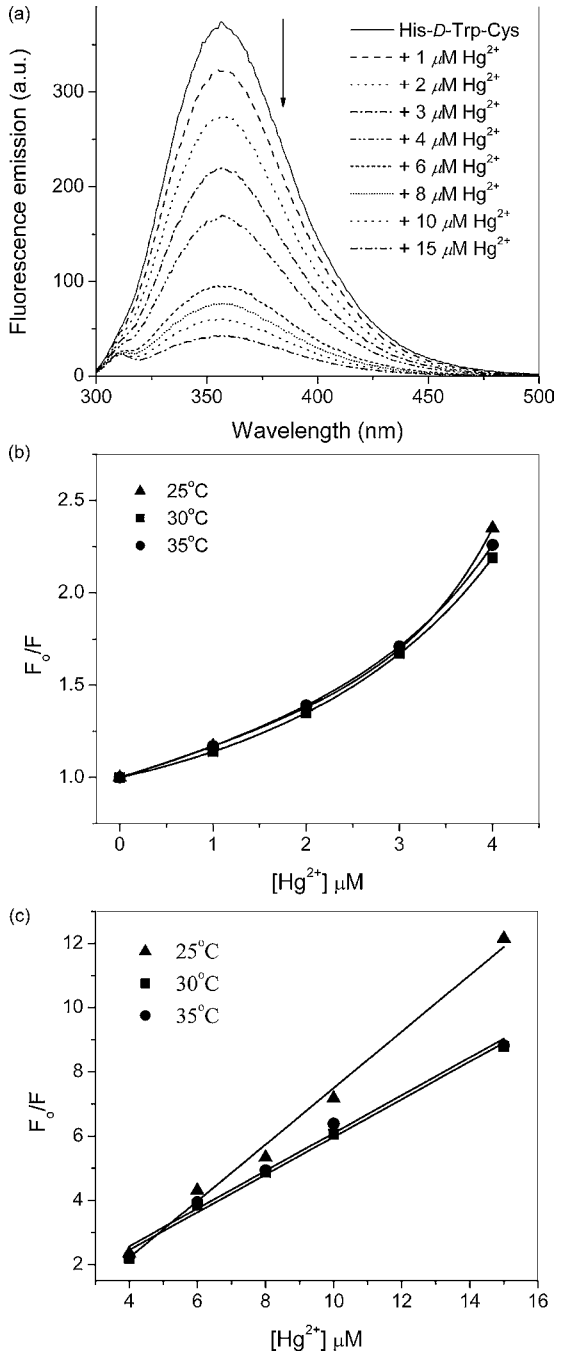

Fig. 5. (a) Fluorescence emission spectrum of 10 μM His-D-Trp-Cys in the absence and presence of increasing concentrations of mercury (II). (b) Stern–Volmer plots for mercury (II) quenching of His-D-Trp-Cys at 25 °C, 30 °C, and 35 °C. Quenching of His-D-Trp-Cys in the presence of less than 5 μM mercury (II), and (c) from 5 μM to 15 μM mercury (II).

3.2. Steady state fluorescence spectroscopy

The effect of mercury (II) on the fluorescence emission intensity of the di-peptide, D-Trp-Cys, is as shown in Fig. 4a. Fluorescence emission of the Trp residue is strongly quenched at low concentrations of mercury (II) and reaches maximum quenching at a mercury (II) to D-Trp-Cys molar ratio of approximately 1.5, which is comparable to ITC data as shown in Fig. 1c. Further analysis of this mercury induced Trp quenching effect by using the Stern–Volmer formalism reveals two different quenching effects (Fig. 4b). In the first stage, at a mercury (II) concentration below 5 μM, the intensity Stern–Volmer plot for quenching by mercury (II) shows a clear upward curvature, concave towards the y-axis, which is characteristic of fluorescence quenching by collisions and complex formation. However, in the second stage, at a mercury (II) concentration greater than 5 μM, which corresponds to the formation of the second complex, the Stern–Volmer plots are linear. When the temperature was raised from 25 °C to 35 °C, the gradient of these linear Stern–Volmer plots decreased (Fig. 4b), corresponding to smaller quenching constants values. The line of best fit analysis of mercury (II) quenching of D-Trp-Cys at greater than 5 μM mercury (II) yielded the linear regression line, $y = 1.50x - 3.28$, $y = 1.11x - 1.49$, and $y = 0.86x - 0.22$, at 25 °C, 35 °C, and 40 °C, respectively, where $r^2 > 0.98$. This type of quenching dependency on temperature (static quenching) is associated with specific binding interactions leading to complex formation. The rationale is that higher temperature will result in the dissociation of weakly bound complexes, and hence smaller amounts of quenching [9b].

The effect of mercury (II) on the fluorescence emission intensity of the corresponding tri-peptide, His-D-Trp-Cys, is similar to that of the di-peptide, D-Trp-Cys. Fig. 5a shows a rapid decrease in the fluorescence emission intensity of His-D-Trp-Cys in the presence of increasing mercury (II) concentrations. Stern–Volmer plots of this fluorescence quenching exhibit two types of bimolecular quenching as shown by D-Trp-Cys. Fluorescence quenching leading to the formation of the first mercury (II) and peptide complex involves both collision and static quenching (Fig. 5b), whereas the second complex formation is associated with static quenching (Fig. 5c). The line of best fit analysis of these linear Stern–Volmer yielded the linear regression line, $y = 8.79x - 1.07$, $y = 5.86x + 0.11$, and $y = 5.88x + 0.22$, at 25 °C, 30 °C, and 35 °C, respectively, where $r^2 \geq 0.99$. When the temperature was raised form 30 °C to 35 °C, there was no further change in quenching constants (Stern–Volmer plots exhibit similar slopes), which suggests the complex is stable at this temperature range.

The dependency of the fluorescence quenching by mercury (II) for D-Trp-Cys and His-D-Trp-Cys corroborates the calorimetric data and support at least two types of sequential complex formations between these peptide ligands and mercury (II).

4. Conclusion

By using calorimetry, we have gained more insight into the origins of binding specificity and affinity in the above system. The first binding interaction between these thiol S-donor peptide ligands and mercury (II) ions is largely due to favorable contribution to the free energy of complexation from the enthalpy term, which indicates significant contributions by mutipolar force and/or dispersive interactions. In the presence of higher mercury (II) concentrations, the free energy of the second binding is compensated by the entropy term, as the solvent reorganization and possibly the conformational changes associated with internal rigidification play a more significant role in stabilizing the complex. As the thiol S-donor peptide ligand increases in size, from di- to tri-peptides, the binding constants decrease as the contribution of the enthalpy term to the

free energy of complexation decreases. However, this can be compensated by increasing the number of thiol S-donor groups in the tri-peptide (for example, Cys-D-Trp-Cys). In summary, these results show that small peptide ligands containing one or more thiol S-donor ligating groups are structurally attractive for the rational design of chelators for mercury (II).

Work is in progress employing density functional theory combined with implicit solvation models to help elucidate probable mercury (II) and peptide complex structures, formation energies, and the effects of solvation. These studies will provide a more detailed description of the complex structures that are present and the significant thermodynamic contributions to the binding constants.

Acknowledgements

The National Science Foundation, grant #CHE 613675, supported this work. S.R. acknowledges support from the NSF HBCU-Undergraduate Program at Winston-Salem State University.

References

[1] O. Andersen, Chem. Rev. 99 (1999) 2683–2710.
[2] H.V. Aposhian, R.M. Maiorino, D. Gonzalez-Ramirez, M. Zuniga-Charles, Z. Xu, J.M. Hurlbut, P. Junco-Munoz, R.C. Dart, M.M. Aposhian, Toxicology 97 (1995) 23–38.
[3] J.R. Campbell, T.W. Clarkson, M.D. Omar, JAMA 256 (1986) 3127–3130.
[4] W.A. Watson, T.L. Litovitz, W. Klein-Schwartz, G.C. Rodgers Jr., J. Youniss, N. Reid, W.G. Rouse, R.S. Rembert, D. Borys, Am. J. Emerg. Med. 22 (5) (2004) 335–404.
[5] C.C. Bridges, R.K. Zalups, Toxicol. Appl. Pharmacol. 204 (2005) 274–308.
[6] C.C. Bridges, C. Bauch, F. Verrey, R.K. Zalups, J. Am. Soc. Nephrol. 15 (2004) 663–673.
[7] M. Aschner, T.W. Clarkson, Brain Res. 462 (1988) 31–39.
[8] T.W. Clarkson, Ann. Rev. Biochem. 32 (1993) 545–571.
[9] (a) J.R. Lakowicz, Principles of Fluorescence Spectroscopy, 3rd ed., Springer Science and Business Media, LLC, New York, 2006, pp. 1–25;
(b) J.R. Lakowicz, Principles of Fluorescence Spectroscopy, 3rd ed., Springer Science and Business Media, LLC, New York, 2006, pp. 278–318.
[10] M. Ngu-Schwemlein, P. Butko, B. Cook, T. Whigham, J. Peptide Res. 66 (s1) (2006) 72–81.
[11] M. Ngu-Schwemlein, W. Gilbert, K. Askew, S. Schwemlein, Bioorg. Med. Chem. 16 (2008) 5778–5787.
[12] J.E. Huheey, E.A. Keiter, R.L. Keiter, Inorganic Chemistry: Principles of Structure and Reactivity, Harper Collins College Publishers, New York, 1993, p. 473.
[13] J.G. Wright, M.J. Natan, F.M. MacDonnell, D.M. Ralston, T.V. O'Halloran, Bioinorganic Chemistry in: S.J. Lippard (Ed.), Progress in Inorganic Chemistry, vol. 38, John Wiley & Sons, New York, 1990, pp. 323–409.
[14] Y. Inoue, T. Hakushi, J. Chem. Soc., Perkin Trans. II (1985) 935–946.
[15] R. Lumry, S. Rajender, Biopolymers 9 (1970) 1125–1227.
[16] E. Grunwald, L.L. Comeford, Thermodynamic mechanisms for enthalpy–entropy compensation, in: R.B. Gregory (Ed.), Protein–Solvent Interactions, Marcel Dekker, New York, 1995, p. 421.
[17] L. Liu, Q.-X. Guo, Chem. Rev. 101 (2001) 673–695.
[18] R.R. Krug, W.G. Hunter, R.A. Grieger, J. Phys. Chem. 89 (1976) 2335–2341, and 2341-2351.
[19] C.P. Woodbury, Introduction to Macromolecular Binding Equilibria, CRC Press, Taylor and Francis Group, LLC, Boca Raton, 2008, p. 7.